

Assembly of synthetic locked chromophores with Agrobacterium phytochromes Agp1 and Agp2

メタデータ	言語: eng 出版者: 公開日: 2017-10-03 キーワード (Ja): キーワード (En): 作成者: メールアドレス: 所属:
URL	http://hdl.handle.net/2297/3030

Assembly of synthetic locked chromophores with *Agrobacterium* phytochromes Agp1 and Agp2

Katsuhiko Inomata^{1*}, Steffi Noack², Mostafa A. S. Hammam¹, Htoi Khawn¹, Hideki Kinoshita¹, Yasue Murata¹, Norbert Michael², Patrick Scheerer³, Norbert Krauss³ and Tilman Lamparter^{2*}

¹Division of Material Sciences, Graduate School of Natural Science and Technology, Kanazawa University, Kakuma, Kanazawa, Ishikawa, 920-1192 JAPAN

²Freie Universität Berlin, Pflanzenphysiologie, Königin Luise Str. 12-16, D-14195 Berlin, Germany

³Charité-Universitätsmedizin Berlin, Institut für Biochemie, Proteinstrukturforschung, Campus Charité-Mitte, Monbijoustr.2, D-10117 Berlin, Germany

Corresponding authors: Prof. Katsuhiko Inomata, Division of Material Sciences, Graduate School of Natural Science and Technology, Kanazawa University, Kakuma, Kanazawa, Ishikawa, 920-1192 JAPAN, Tel: +81-76-264-5700, Fax: +81-76-264-5742, E-Mail:

inomata@cacheibm.s.kanazawa-u.ac.jp

Tilman Lamparter, Freie Universität Berlin, Pflanzenphysiologie, Königin Luise Str. 12-16, D-14195 Berlin, Tel: +49 30 838 54918, FAX +49 30 838 54357, E-Mail: lamparte@zedat.fu-berlin.de

Phytochromes are photoreceptors with a bilin chromophore in which light triggers the conversion between the red-absorbing form Pr and the far-red-absorbing form Pfr. *Agrobacterium tumefaciens* has two phytochromes, Agp1 and Agp2, with antagonistic properties: in darkness, Agp1 converts slowly from Pfr to Pr, whereas Agp2 converts slowly from Pr to Pfr. In a previous study, we have assembled Agp1 with synthetic locked chromophores 15Za, 15Zs, 15Ea, 15Es, in which the C15=C16 double bond is fixed in either the *E* or *Z* configuration and the C14-C15 single bond in either the *syn* (*s*) or *anti* (*a*) conformation. In the present study, the locked chromophores 5Za and 5Zs were used for assembly with Agp1; in these chromophores, the C4=C5 double bond is fixed in the *Z* configuration and the C5-C6 single bond in either the *syn* or *anti* conformation. All locked chromophores were also assembled with Agp2. The data show that in both phytochromes, the Pr chromophore adopts a C4=C5 *Z* C5-C6 *syn* C15=C16 *Z* C14-C15 *anti* stereochemistry and that in the Pfr chromophore the C15=C16 double bond has isomerized to the *E* configuration, whereas the C14-C15 single

bond remains in the *anti* conformation. Photoconversion shifted the absorption maxima of the 5Zs adducts to shorter wavelengths, whereas the 5Za adducts were shifted to longer wavelengths. Thus, the C5-C6 single bond of the Pfr chromophore is rather in an *anti* conformation, supporting the previous suggestion that during photoconversion of phytochromes, a rotation around the ring A-B connecting single bond occurs.

Almost all organisms have adopted mechanisms to sense light via photoreceptors and respond to different light conditions in manifold ways. Phytochromes are photoreceptors that are reversibly converted by light between two stable or long lived forms, the red-absorbing Pr¹ and the far-red-absorbing Pfr (1). Depending on the species, phytochromes bind one of three bilins as a chromophore: land plants utilize phytychromobilin (PΦB) (2), cyanobacteria use phytycyanobilin (PCB) (3; 4) whereas all other organisms including proteobacteria and fungi use biliverdin (BV) (5-7). The chromophore is covalently attached to a cysteine residue during an autocatalytic process. Whereas plant and cyanobacterial phytochromes use a cysteine in the so called GAF domain of the protein as chromophore attachment site (2), the chromophore binding cysteine of BV-binding phytochromes is close to the N-terminus of the protein (8-10). NMR studies with plant phytochromes showed that the chromophore undergoes isomerization around the double bond connecting the rings C and D during photoconversion from Pr to Pfr (11). The configuration of this double bond is *Z* in the Pr and *E* in the Pfr form. Time resolved spectroscopy techniques show that this *Z-E* isomerization, leading to the lumi-R photoproduct, takes place on a picosecond time scale (12; 13). Later intermediates, termed meta-Ra, meta-Rb and meta-Rc, as well as the photoproduct Pfr are formed in the microsecond and millisecond time frame (14; 15). For the reverse photoreaction from Pfr to Pr, a scheme starting with the formation of lumi-F, which is formed by a rapid C15=C16 *E* to *Z* isomerization followed by intermediates, has been proposed (16; 17). Most information on the configuration and conformation of the chromophore is available for the Pr form, for which a clear picture has been obtained recently from the crystal structure of the chromophore-binding-domain of *Deinococcus* phytochrome DrBphP (10). However, detailed knowledge of configurational and conformational changes of the chromophore that are reflected by spectral changes is lacking. Four different synthetic locked chromophores, in which the rings C and D are held in a fixed orientation by an additional carbon chain, have been assembled with phytochrome Agp1 from *Agrobacterium*

tumefaciens (18). In these chromophores, termed 15Za, 15Zs, 15Ea and 15Es, the double bond is either in the *Z* or *E* configuration and the single bond either in the *syn* (*s*) or *anti* (*a*) conformation. All chromophores were incorporated into the protein and formed covalently linked photostable adducts. UV/vis spectra of the 15Za adduct were comparable with the Pr form of BV-Agp1, whereas the 15Ea adduct resembled the Pfr form. Both the 15Zs and 15Es adducts absorbed only in the blue region of visible light. These data show that the C15=C16 double bond switches from the *Z* to the *E* configuration upon photoconversion from Pr to Pfr, which is in line with previous assumptions, and that the C14-C15 single bond has an *anti* conformation throughout the entire photocycle (18). The latter notion is in contrast with former studies that predicted a rotation around the C14-C15 single bond during Pr to Pfr conversion (19), but in line with recent density functional theory (DFT) calculations combined with Resonance Raman spectroscopy (20). The crystal structure of the chromophore-binding domain of *Deinococcus* phytochrome shows that a rotation around the C14-C15 single bond would be hindered by the surrounding amino acids and supports the *anti* conformation of the C14-C15 single bond in both the Pr and Pfr forms. Size exclusion chromatography (SEC) and phosphorylation studies showed that the 15Za and 15Ea adducts adopt a protein conformation that is comparable with the Pr and Pfr forms of the BV-adduct, respectively (18). Direct information on the configuration of the C4=C5 and C9=C10 double bonds has been lacking. Most researchers have predicted that the C4=C5 double bond is always in the *Z* configuration, whereas both *E* and *Z* configurations have been proposed for the C9=C10 double bond (20; 21). The crystal structure showed that in the Pr form both double bonds are in the *Z* configuration. Conflicting results have also been obtained for the conformation of the C5-C6 single bond. The interpretation of the Resonance Raman spectra of plant phytochromes by DFT calculations suggested an *anti* conformation in the Pr and a *syn* conformation in the Pfr form (20). The crystal structure showed that in the Pr form of DrBphP, this single bond is in the *syn* conformation. As noted above, plant

phytochromes (with a PΦB chromophore) and BV-binding phytochromes have different chromophore attachment sites. The ring A ethylidene or vinyl side chain, respectively, is involved in covalent bond formation. The crystal structure predicts that the position of both chromophore binding cysteines would be on opposite sides of the side chains. It could therefore be that in the Pr form of phytochromes, both C5-C6 conformations are realized: *syn* for BV-binding and *anti* for PCB- and PΦB-binding species. However, the conformation of the C5-C6 single bond of plant phytochromes has still to be established. Whether or not photoconversion involves a rotation around the C5-C6 single bond, as evidenced by DFT calculations (20), is also unclear.

Whereas Agp1 of *A. tumefaciens* converts from Pfr to Pr in darkness, a feature well known from many plant phytochromes, the second phytochrome of *A. tumefaciens*, Agp2, converts from Pr to Pfr in darkness (22). Such a property has also been found for three other BV-binding phytochromes from the bacteria *Bradyrhizobium spec.* (23), *Rhodopseudomonas palustris* (24) and *Pseudomonas aeruginosa* (25). Physiological evidence suggests that a similar phytochrome exists in the slime mold *Physarum polycephalum* (26). Based on spectral similarities, it may be predicted that the dark conversion of these phytochromes is initiated by the same C15=C16 *Z-E* isomerization as during photoconversion from Pr to Pfr of typical phytochromes, but direct evidence is lacking. In free bilins, the *ZZZ* configuration is the thermodynamically stable configuration (27; 28). Within a small group of phytochromes, the protein environment seems to make the C15=C16 *E* configuration thermodynamically more favorable.

To see whether and how locked chromophores are incorporated into Agp2, the set of the above mentioned chromophores was also tested with purified recombinant Agp2. For analyses on the stereochemistry of the C5-C6 single bond, new locked 5Za and 5Zs chromophores were used for assembly with Agp1 and Agp2. These studies provided deeper insight into the similarities and differences between a more conventional phytochrome and a phytochrome that converts to Pfr in darkness and give further clues for the

understanding of chromophore stereochemistry in the ground state and during photoconversion.

EXPERIMENTAL PROCEDURES

Expression and purification of Agrobacterium phytochromes Agp1 and Agp2 - An *E. coli* expression vector termed pAG1 was used for full length Agp1. pAG1 encodes for the Agp1 protein with a C-terminal poly-histidine tag for Ni²⁺ affinity purification (8). For recombinant Agp2, a pET21b (Novagen) derived expression vector as described in (28) was used. The vector was modified to encode for a C-terminal histagged protein; expression, purification and assembly were performed as for Agp1. Another expression vector, pAG1-M15, encodes for the N-terminal 504 amino acids and a his-tag (29). The expressed protein is termed Agp1-M15. For expression and purification of Agp1, Agp1-M15 and Agp2 apoproteins, we followed the same procedure as described previously (8). In brief: *E. coli* cells harboring the expression plasmid were grown in rich broth medium. Specific protein expression was induced by IPTG, and the cells were disrupted with a French pressure cell. Soluble proteins were purified by Ni²⁺ affinity chromatography and by preparative SEC. The SEC was performed in "basic buffer" (300 mM NaCl, 50 mM Tris/Cl, 5 mM EDTA, pH 7.8). The final apoprotein concentration was ca. 15 mg/ml. At this stage, the protein was stored at -80 °C.

Synthesis of Bilin Derivatives - Biliverdin (BV) was purchased from Frontier Scientific (Carnforth, U.K.). Synthesis of 18EtBV was performed according to the protocols published for PΦB, PCB, and PCB derivatives (30-33). 15Za [UV/vis (MeOH) λ_{\max} 385 (ϵ = 23,355), 645 (ϵ = 17,729) nm], 15Zs [UV/vis (MeOH) λ_{\max} 383 (ϵ = 39,850), 639 (ϵ = 18,650) nm], 15Ea [UV/vis (MeOH) λ_{\max} 381 (ϵ = 40,533), 630 (ϵ = 29,260) nm] and 15Es [UV/vis (MeOH) λ_{\max} 389 (ϵ = 33,000), 648 (ϵ = 13,567) nm] derivatives were prepared as reported (34-36). Syntheses of 5Za [UV/vis (MeOH) λ_{\max} 383 (ϵ = 12,633), 644 (ϵ = 11,067), 719 (ϵ = 7,533) nm] and 5Zs [UV/vis (MeOH) λ_{\max} 389 (ϵ = 26,533), 637 (ϵ = 8,333) nm] will be published elsewhere. Bilin stock solutions of ca. 1 mM concentration, judged from the weight of the dissolved solid

compounds, were prepared in dimethylsulfoxide (DMSO) and stored at -80 °C. The exact concentration of each stock solution was estimated by UV/vis spectroscopy.

Assembly and UV/vis spectroscopy - UV/vis spectra were recorded as before (8) at 18 °C. The concentration of apoproteins was estimated from the absorbance at 280 nm. A precise concentration of the bilin stock solution was estimated from the absorbance of the diluted solution of an aliquot in MeOH based on the corresponding molecular extinction coefficient (ϵ) of each locked chromophore described above. For assembly studies, the apoprotein was diluted with basic buffer to a final concentration of ca. 10 μ M and pipetted into a measuring cuvette. After addition of 1 mM (final concentration) tris(2-carboxyethyl)phosphine, chromophore was added from the DMSO stock solution to a final concentration of ca. 5 μ M; the sample was mixed rapidly for 30 s. Immediately after mixing, a spectrum was recorded from 900 to 250 nm; the duration of the scan was ca. 1 min. Nine further spectra were recorded in 5 min intervals. Series of 10 spectra with various time intervals were recorded until absorbance changes were apparently complete. The time intervals between subsequent measurements were 10 min, 30 min and 60 min for the second, third and fourth measuring series. To analyze whether chromophores are covalently bound to the protein, apoprotein and chromophore were mixed as above and incubated until assembly was complete. Thereafter, SDS was added to a final concentration of 1% and the sample was incubated again for 10 min. The mixture was passed over a desalting column as described previously (8). From a comparison of absorption spectra before and after column separation, the amount of covalently bound chromophore can be estimated. For photoconversion of Pr to Pfr or Pr to Pnr (the near red absorbing form), the samples were irradiated with red light from a light emitting diode ($\lambda_{\text{max}} = 655$ nm; halfbandwidth = 40 nm); the light intensity was 135 $\mu\text{mol m}^{-2} \text{s}^{-1}$ at the position of the cuvette. For photoconversion of Pfr to Pr, the sample was irradiated with a 785 nm laser diode (RLD-78MA, Sanyo; halfbandwidth = 10 nm); the light intensity was 70 $\mu\text{mol m}^{-2} \text{s}^{-1}$ at the position of the cuvette. For irradiations with orange light, the light beam of a halogen projector was passed

through an AL interference filter (Schott, Mainz, Germany, $\lambda_{\text{max}} = 608$ nm; halfbandwidth = 40 nm); the light intensity was 45 $\mu\text{mol m}^{-2} \text{s}^{-1}$ at the position of the cuvette. Dark reversion and photoconversion kinetics were measured with the time drive program of the photometer in which the measuring wavelength was set to λ_{max} of the Q-band of the Pr form (around 700 nm). The initial rate of back-conversion in darkness or under illumination was estimated from the derivative. This value was divided by the initial light induced absorbance change of a dark assembled sample, i.e. the value that corresponds to the concentration of the photoproduct.

Analytical size exclusion chromatography - The Agp1-M15 apoprotein (10 μ M) was mixed with BV, 5Za or 5Zs (ca. 15 μ M) and incubated for ca. 3 h. The adducts were used either unirradiated ("Pr") or after saturating red irradiation ("Pfr"). Analytical SEC was carried out in darkness on a Superdex 200 HR 10/30 column (Amersham/Pharmacia, Freiburg, Germany) as described previously (18). The elution was monitored at 280 nm.

RESULTS

Chromophores that were used in the present study are shown in Fig. 1. Biliverdin (BV), which is the natural chromophore of *A. tumefaciens* phytochromes, was used as control. The synthetic derivative 18-Ethyl-BV (18EtBV) was used as a second control. This compound is distinguished from BV by the side chain at C18 position of the bilin skeleton, which is an ethyl group in the former and a vinyl group in the latter. For technical reasons, the locked chromophores have also an ethyl group at C18. The nomenclature of the locked chromophores is also given in Fig. 1. The number 5 or 15 stands for the C-atom of the methine bridge which is held in a sterically fixed orientation by an additional carbon chain, the first letter stands for the configuration of the methine bridge double bond and the second letter for the conformation of the single bond (*s* for *syn* and *a* for *anti*). Both phytochromes of *A. tumefaciens*, which are termed Agp1 and Agp2 (or AtBphP1 and AtBphP2 by other groups), were used for studies on chromophore assembly and photoconversion. The chromophores 15Za, 15Zs, 15Ea and 15Es

have been tested with Agp1 in a previous study (18). The present work extends the Agp1 studies by 5Za and 5Zs. In addition, the "unusual" phytochrome Agp2 was also assembled with all presently available locked chromophores.

Assembly of Agp1 with 5Za and 5Zs - Figure 2 shows series of UV/vis spectra that were measured during 51 min after mixing Agp1 apoprotein with 5Za (Fig. 2 a) and 5Zs (Fig. 2 b) in comparison with the spectra of the free chromophores. For both 5Za and 5Zs, absorption changes were observed that are characteristic for chromophore assembly and show that these compounds are also incorporated into the chromophore pocket. The absorption maxima of the 5Za and 5Zs adducts were at 672 and 692 nm, respectively. In Fig. 3, the time courses of absorbance values are presented together with the values obtained with those chromophores that had already been analyzed in the previous study (18). This comparison shows that the 5Za assembly is faster than the 5Zs assembly and that both chromophores assemble faster than 15Ea but slower than BV, 18EtBV, 15Za, 15Zs and 15Es. After an incubation time of 2 h, both the 5Za and 5Zs chromophores were covalently bound to the protein, as judged by desalting column tests with SDS-treated holoprotein (data not shown).

Photoconversion of 5Za-Agp1 and 5Zs-Agp1 - All Agp1 adducts with the chromophores in which the rings C and D are sterically locked did not undergo light-induced absorption changes (18). Phytochrome photoconversion is initiated by a Z to E isomerization around the C15=C16 double bond, which is not possible in these adducts. In the 5Za and 5Zs adducts, this isomerization is not hindered. Therefore, irradiation should result in absorption changes. After irradiating the 5Za adduct with red light, the absorbance around 672 nm was reduced, accompanied by an increase in the longer wavelength region, and a band broadening in the wavelength region around 370 nm (Fig. 4 b). Obviously, the Pr-like form converts partially into a Pfr-like form which absorbs at higher wavelengths and has a rather low extinction coefficient.

Irradiation of the 5Zs adduct resulted in a shift of the maximum by 56 nm towards shorter

wavelengths (from 692 nm to 636 nm), and a reduction of absorbance in that spectral region (Fig. 4 c). Thus, photoconversion shifts the absorption maximum of this adduct to the opposite direction than the adducts with BV (18), 18EtBV (Fig. 4 a) and 5Za (Fig. 4 b). Light-induced absorbance changes of 5Zs-Agp1 resemble closely those of the unusual bacteriophytochrome BphP3 of *Rhodospseudomonas palustris*, in which the absorption maximum shifts by 60 nm from 705 nm to 645 nm upon irradiation (37). The photoproduct of RpBphP3 has been denominated "Pnr", where "nr" stands for "near red" light. In accordance with this nomenclature, we also denominate the photoproduct of the Agp1-5Zs adduct as Pnr.

It has been shown that BV-Agp1 converts from Pfr to Pr in darkness and that the quantum yield of the light-induced Pfr to Pr conversion is rather low (8). In the present study, we performed comparative measurements on dark reversion and light-induced back-conversion with BV-Agp1, 18EtBV-Agp1, 5Za-Agp1 and 5Zs-Agp1 (Table 1). The initial rate of dark reversion of the BV adduct was $2.2 \cdot 10^{-3} \text{ s}^{-1}$, the initial rate of Pfr to Pr conversion under rather strong 785 nm light was about twice as high as that of the dark reversion.

Dark reversion of 18EtBV-Agp1 was about 10 times slower than that of the BV-adduct. Note that the only difference between BV and 18EtBV is a substituent at the C18 position; the vinyl group in BV is replaced by an ethyl group in 18EtBV. This is the same difference as between PΦB and PCB, which are natural chromophores of plant and cyanobacterial phytochromes, respectively. It has been observed that the PΦB-adduct of cyanobacterial phytochrome Cph1 undergoes dark reversion, whereas dark reversion of the PCB-adduct was negligible (38). The initial rate of the 18EtBV-Agp1 Pfr to Pr conversion in the presence of 785 nm light was also about 10 times lower than that of the BV-adduct. The extinction coefficient of the 18EtBV-adduct at 785 nm is about 3 times lower than that of the BV-adduct. Based on these data, it may be concluded that the quantum yield of the light-induced Pfr to Pr conversion of 18EtBV-Agp1 is about 2 times lower than that of the BV-adduct.

The Pfr-like photoproduct of 5Za-Agp1 undergoes a dark reversion which is about 30 times faster than that of the 18EtBV adduct. In the presence of strong 785 nm light, the initial rate of back conversion was slightly below the dark reversion. This result shows that 785 nm light triggers a "Pr" to "Pfr" photoconversion, thereby slowing down the dark reversion. Due to the rather high rate of dark reversion, it is unclear whether a "Pfr" to "Pr" photoconversion occurs. However, it is clear that the quantum yield of this photoreaction must be very low or zero.

The dark conversion of 5Zs-Agp1 from Pnr to Pr is rather slow (Table 1). In the presence of orange light of 608 nm, which is more absorbed by the Pnr than by the Pr form, the dark reaction is slowed down by a factor of 2. Thus, orange light triggers rather Pr to Pnr photoconversion than the reverse reaction. The quantum yield of the Pnr to Pr photoconversion must also be very low or zero.

We also performed SEC studies with 5Za and 5Zs Agp1-M15 adducts. The Agp1-M15 deletion mutant contains the photosensory module of Agp1 with the PLD, GAF and PHY domains, but lacks the histidine kinase module (29). The BV adduct of Agp1-M15 undergoes light-induced conformational changes that can easily be monitored by SEC. In the Pfr form, the holoprotein has a higher SEC mobility than in the Pr form. The same result was obtained with the 18EtBV adduct; the 15Za adduct elutes like Pr and the 15Ea adduct like Pfr (18). Ongoing studies showed that the light-induced mobility changes are due to differential subunit interactions. At the protein concentration of 10 μ M, BV-Agp1-M15 exists as monomer, dimer, trimer and tetramer in both the Pr and Pfr forms, but dimerisation is more preferred in the Pfr form. The differential SEC mobility reflects the different degree of dimerisation (S. Noack and T. Lamparter, unpublished). In the present study, we found that the unirradiated 5Za and 5Zs adducts elute like the Pr form of the BV-adduct (Fig. 5). Photoconversion changed the elution profile of both adducts. The mobility of the 5Zs adduct was only slightly affected. Its elution maximum was at 13.9 ml in the Pnr and at 13.7 ml in the Pr form, whereas with BV-Agp1-M15 the elution maximum was 13.8 ml in the Pr and 13.2 ml in the Pfr form. The elution profiles in

Fig. 5 are normalized in such a way that the areas under the curves are identical. In this way, the amplitude gives an indirect impression of the broadness of the elution peak. The elution peaks of BV-Agp1-M15 Pfr and 5Zs-Agp1-M15 Pnr are slightly broader than those of the Pr forms. The Pfr-like form of the 5Za adduct had an unusual elution pattern. The elution peak was centered on the peak of the unirradiated adducts, but was much broader than all other elution profiles of the present study. The reason for the broad profile is unclear, but it might indicate that the protein undergoes partial denaturation upon irradiation. It should be stressed that neither the photoconverted 5Zs nor the 5Za adduct is comparable with the Pfr form of the BV-adduct.

Assembly of Agp2 with BV, 18EtBV, 15Za, 15Zs, 15Ea, 15Es, 5Za and 5Zs - Biliverdin assembly of Agp2 is accompanied by dark conversion from Pr to Pfr ((22) and Fig. 6 a). The same feature was found for the assembly of 18EtBV with Agp2 (Fig. 6 b). In Fig. 7, the time course of absorbance changes at the positions of the Pr and the Pfr absorption maxima is given for both chromophores. With the BV chromophore, the maximum Pr absorbance was obtained directly (1 min) after mixing, showing that chromophore protein interaction is a rapid process. With the 18EtBV chromophore, a high Pr absorbance was also obtained at $t = 1$ min, but the value increased slightly until $t = 6$ min and declined thereafter as the result of dark conversion. The Pr absorbance increase probably reflects the transition from non-covalent to covalent binding, as in Agp1, and implies that covalent bond formation is possible in the Pr form. The comparison between BV and 18EtBV shows that both assembly and dark conversion are slower with the 18EtBV than with the BV chromophore. It should be stressed that in the Agp2 adducts, the ring D side chain (vinyl in BV or ethyl in 18EtBV) has qualitatively the same impact on the rate of dark conversion as in the case of Agp1, although dark conversions of Agp1 and Agp2 adducts proceed in opposite directions. All locked chromophores used in the present study were also incorporated into the Agp2 apoprotein. This was shown by absorbance changes that occur after mixing chromophores with the protein (Fig. 6 c-h and Fig. 8). It was shown by SDS-desalting column tests that after

completion of absorbance changes, all chromophores were covalently bound to the protein (data not shown). However, for none of the locked chromophores was the assembly accompanied by dark conversion into another form. The 15*Za* and 15*Ea* adducts were comparable with the corresponding Agp1 adducts and spectrally similar to the Pr and Pfr form, respectively. The assembly of 15*Za* with Agp2 was much slower than that of 15*Ea*, BV or 18EtBV. The absorbance increase of the former was completed after an incubation time of ca 24 h, whereas assembly with the other three chromophores was completed after 60 to 300 min (Fig. 7 and Fig. 8). The data of the 15*Za* chromophore show again that covalent bond formation is also possible in the Pr form, whereas the low rate of assembly implies that this chromophore does not fit well into the chromophore pocket of the Agp2 apoprotein and the complete assembly requires marked conformational changes.

Incorporation of 15*Zs* and 15*Es* occurs again very rapidly; the chromophore absorption spectra changed immediately ($t = 1$ min) after mixing with no significant further change thereafter. The adducts have absorption maxima in the blue wavelength region and are thus similar to the corresponding Agp1 adducts.

The 5*Zs* assembly with Agp2 produced a similar Pr-like adduct as with Agp1. The fact that the 5*Zs*-Agp2 adduct shows no dark conversion into a Pfr-like form is remarkable, since a *Z* to *E* isomerization around the C15=C16 double bond is most likely the initial step of BV-Agp2 dark conversion. This isomerization would not be hindered in the 5*Zs*-Agp2 adduct. Assembly of 5*Za* with Agp2 is comparable with the 5*Za*-Agp1 assembly described above insofar as an absorption band in the 700 nm region is formed immediately after mixing and decays thereafter. It should however be mentioned that Agp2 assembles much faster with 5*Za* than with 5*Zs*. This might indicate that 5*Za* fits better into the chromophore pocket of Agp2 than 5*Zs*. The final Agp2-5*Za* adduct has an absorption maximum at 640 nm, which is lower than the 672 nm of the Agp1 adduct. There is also no apparent dark conversion in the 5*Za*-Agp2 adduct during assembly, unless the absorbance decrease around 700 nm is considered as an indication for dark-conversion.

Photoconversion of Agp2 adducts - The 15*Za*, 15*Zs*, 15*Ea* and 15*Es* adducts with Agp2 revealed no photoconversion (data not shown), in accordance with the corresponding Agp1 adducts (18). Spectra of the BV, 18EtBV, 5*Za* and 5*Zs* adducts with Agp2 before and after irradiation are given in Fig. 9. Irradiation of BV- and 18EtBV-Agp2 with far-red light yielded similar Pr-like photoproducts (Fig. 9 a, b). There is however a qualitative difference between them: The relative absorbance of 18EtBV-Agp2-Pr is significantly higher than that of BV-Agp2-Pr. Consequently, the difference spectrum of the 18EtBV adduct has a more typical phytochrome-like shape than that of the adduct with the natural BV chromophore.

Quite interestingly, photoconversion of 5*Zs*-Agp2 is again comparable with that of 5*Zs*-Agp1: irradiation resulted in a blue shift of the absorption maximum from 692 to 675 nm to the "Pnr" form (Fig. 9 d). The special feature of Agp2 is thus completely lost in the 5*Zs* adduct. Irradiating the 5*Za* adduct resulted in a subtle absorption increase around 700 nm (Fig. 9 c). Thus, a fraction of the 5*Za* adduct seems to convert to a form that absorbs at longer wavelengths. In this respect, photoconversion of 5*Za*-Agp2 also reminds of the Pr to Pfr photoconversion, although the overall shape of the photoproduct spectrum is significantly different from the Pfr spectrum of the BV- or 18EtBV adducts.

We also tested the Agp2 adducts for dark reversion and the effect of light on the back reaction (Table 2). The qualitative difference that was found for the Pr to Pfr dark conversion during the assembly of Agp2 with BV and 18EtBV was also found after Pfr to Pr photoconversion of the adducts. With an initial rate of $1.2 \cdot 10^{-2} \text{ s}^{-1}$, BV-Agp2 revealed the fastest dark reversion of the present study. The value of 18EtBV-Agp2 was ca. 3 times lower. For both adducts, the Pr to Pfr conversion was significantly accelerated by irradiation with 655 nm light. Although the quantum yield of photoconversion was not exactly estimated in this study, the comparison with the initial rate of Pr to Pfr photoconversion of BV-Agp1 ((8) and data not shown) implies that the photoconversion quantum yields of both Agp2 adducts are in the range of 10%, i.e. in the range of normal

phytochromes (see (8) for a discussion on quantum yields).

Due to the low absorption changes of 5Za-Agp2, rates of dark reversion or light driven back-conversion could not be measured. Pnr to Pr dark reversion of 5Zs-Agp2 was rather slow. In the presence of 608 nm light, the initial rate of Pnr to Pr reversion was ca. 3 times higher (Table 2). Therefore, light triggers both Pr to Pnr and Pnr to Pr conversion of this adduct.

DISCUSSION

The combination of Agp1 and Agp2 on the one side and the extended collection of locked chromophores on the other side for assembly and photoconversion studies revealed a deeper insight into the spectral properties of phytochromes. Agp1 and Agp2 are phytochromes from the same species, but rather distantly related to each other. Properties common to both phytochromes might point to general principles at least for the group of biliverdin-binding phytochromes, the evolutionarily more ancient ones. Since all chromophores used in the present study formed covalent adducts with both phytochromes, we predict that also other phytochromes will incorporate the same or similar locked chromophores, given that the requirements for the reacting ring A C3 side chain are met by the chromophore - vinyl for BV binding phytochromes and ethylidene for PCB and PΦB binding phytochromes. We found that Agp1 and Agp2 form spectrally similar adducts with the chromophores 15Za, 15Zs, 15Ea, and 15Es, in which the rings C and D are sterically locked. The 15Za adduct spectra resemble those of the Pr form and the 15Ea adduct spectra are similar to those of the Pfr form, whereas the 15Zs and 15Es adducts absorb in the blue wavelength region. The latter feature is either explained by a reduced C9=C10 double bond or by a helical conformation of these chromophores in the protein pocket.

It has previously been found that 15Zs and 15Es are rapidly incorporated into Agp1 and that the adducts have unusual absorption characteristics with maxima in the blue. A more detailed analysis (Fig. 3) showed that both chromophores are more rapidly assembled with the protein than the corresponding unlocked chromophore

18EtBV. Moreover, the data of Fig. 6 f, h and Fig. 8 show that the assembly of 15Zs and 15Es with Agp2 is also very rapid and that the absorption maxima of both adducts are comparable with the Agp1 adducts. The structure of DrBphP implies that a bilin with a C14-C15 *syn* geometry would not exactly fit into the chromophore pocket because ring D would clash with the surrounding amino acids. We therefore propose that the rings C and D, which are linked by the additional carbon chain, might be displaced in the 15Es and 15Zs adducts. A torsional deformation at the C10-C11 single bond, which would result in an increased angle between the planes of rings AB and CD, would break the conjugation between the π -electron systems of the two chromophore halves. With such an arrangement, an absorption maximum in the blue spectral region is expected, as has been shown by chemical modification of the C10-carbon atom of a free bilin (27;39). Thus, an angle greater than 30° between rings AB and CD would explain the blue absorption maxima of the 15Zs and 15Es adducts. The rapid assembly of 15Zs and 15Es might indicate that except for the covalent thioether linkage, the binding modes of these chromophores and the other natural or locked chromophores are very different, and that assembly of 15Zs and 15Es is characterized by smaller activation energies. The spectral shift of the 15Zs and 15Es adducts during assembly could also be explained by addition of a nucleophile to the C10 atom of the chromophore, which also splits the π -electron system, as noted before (18).

Interesting differences between Agp1 and Agp2 and between different chromophores were found for the assembly rates, reflecting either different initial association constants or different initial distances between the ring A vinyl side chain and the sulfur of the chromophore binding cysteine residue. The slowest assembly with Agp1 was found for the 15Ea chromophore. A reasonable explanation for this fact could be that chromophore protein interaction requires slow conformational changes or that the initial distance between chromophore-binding cysteine and the ring A vinyl side chain is rather large. Indeed, the 15Ea-Agp1 holoprotein adopts a Pfr-like conformation as judged by SEC and autophosphorylation studies (18), i.e. the holoprotein has undergone conformational

changes during the assembly process. In the case of Agp2, the 15*Ea* assembly rate is faster than that of 15*Za*. In view of one of the above models, the initial vinyl-cysteine distance would be larger for 15*Za* than for 15*Ea*. The assembly rates for 15*Ea*/15*Za* for both phytochromes are in line with the finding that Agp1 adopts a Pr form and Agp2 a Pfr form in darkness.

Results with the 5*Za* and 5*Zs* chromophores may be summarized as follows. (i) Both chromophores form covalent bonds with either Agp1 or Agp2. (ii) The spectra and the absorption maxima of the 5*Zs* adducts are similar to those of the Pr form of the 18EtBV control. (iii) The absorption spectra of the 5*Za* adducts are also similar to Pr, but their maxima are shifted to shorter wavelengths. (iv) Irradiation of the 5*Zs* adducts induces a blue shift, whereas the 5*Za* adducts are red shifted. Therefore, the irradiated 5*Za* adducts are spectrally more similar to the Pfr form than the 5*Zs* adducts. (v) There is no or a very inefficient photoconversion from the Pnr to the Pr form of 5*Zs*-Agp1. The same holds for the Pfr-like to Pr photoconversion of 5*Za*-Agp1.

All data that were obtained with these chromophores lead to the conclusion that a flexibility around the ring-A/B connecting methine bridge is essential for proper photoconversion from Pr to Pfr and for Pr to Pfr dark conversion of Agp2, although the role of C15=C16 *Z-E* isomerization as the initial step is not questioned by our results.

The spectral analogy between Pr and the 5*Zs* adducts is in line with the data from the crystal structure of the chromophore binding domain of *Deinococcus* phytochrome. In this structure, the configuration / conformation of the BV chromophore is 5*Zs*/10*Zs*/15*Za*, i.e. the single bond between the rings A and B is in the *syn* conformation. DrBphP is found to be useful as a structural model for Agp1 in this context because most amino acid residues which define the chromophore binding pockets are conserved between these proteins. With the coordinates of DrBphP, we tested by modeling whether and how the locked 5*Za* and 5*Zs* chromophores would fit into the chromophore pocket (Fig. 10). These analyses showed that the protein gives enough space for the ring A of both locked chromophores and also that a covalent bond between the ring A vinyl side chain and the

chromophore-binding cysteine can be formed. The modeling results and the data obtained with 5*Za* and 5*Zs* thus show that a rotation around the C5-C6 single bond, which has been predicted to occur during Pr-Pfr photoconversion of plant phytochromes (20), is in principle possible and not restricted by the protein.

The absorption changes during Pr to Pfr transition are more similar to light induced absorption changes of the 5*Za* adducts than to those of the 5*Zs* adducts. This implies that in the Pfr form, the C5-C6 single bond is indeed in the *anti* and not in the *syn* conformation. As outlined above, the 5*Za* photoproducts are however spectrally not exactly identical with Pfr. In addition, the gross protein conformation of the 5*Za*-Agp1-M15 photoproduct is also different from that of Pfr, as shown by SEC. Thus, the 5*Za* model does not precisely reflect the configuration / conformation of the Pfr chromophore. We consider three different explanations for these discrepancies. (i) According to the crystal structure of DrBphP, the ring A nitrogen forms hydrogen bonds with an oxygen atom of the protein backbone and with a water molecule. This hydrogen bond network extends to the ring B and C nitrogen atoms. The chromophore in the Pr and Pfr forms is protonated, and undergoes transient deprotonation upon photoconversion. In 5*Za*, the ring A nitrogen is connected to the additional carbon chain which is used for the fixation. Therefore, this nitrogen can not be part of a hydrogen bond network. This disturbance could explain the spectral dissimilarities between Pfr and the photoconverted 5*Za* adducts. (ii) The Pfr chromophore might adopt a conformation which requires torsions between rings A and B that are not possible with the locked chromophore. (iii) There is also the possibility that an isomerization around the C4=C5 double bond occurs during the photoconversion from Pr to Pfr. Such an isomerization would be blocked in the 5*Za* chromophore. To our knowledge, there is as yet no evidence for a C4=C5 *E* configuration of the Pfr chromophore (11). However, such a configuration might have been overlooked for chemical or technical reasons. In the next step, we intend to synthesise the locked 5*Ea* and 5*Es* chromophores and test these compounds for assembly with phytochrome. Consequently, based on the above results, we propose that the

stereochemistry of the Agp1 and Agp2 chromophores is 5Zs/10Zs/15Za in the Pr and 5Ea/10Zs/15Ea or 5Za/10Zs/15Ea in the Pfr form. A schematic presentation of the proposed stereochemistry of Pr and Pfr is given in Fig. 11. The data of 5Zs-Agp1 and 5Zs-Agp2 adducts show that photoconversion results in a blue shift if the methine bridge between rings A and B of

the natural chromophore is locked. This light-induced blue shift is very similar to the blue shift that has been observed with BphP3 from *Rhodospseudomonas palustris* (37). Therefore, the unusual behavior of RpBphP3 can be explained if in the chromophore pocket of this protein, the rings A and B are held in a tight position each other.

REFERENCES

1. Tu, S. L. and Lagarias, J. C. (2005) In: The Phytochromes. Briggs, W. R. and Spudich, J. L., editors. *Handbook of Photosensory Receptors*, Wiley Verlag, Weinheim, Germany
2. Rüdiger, W. and Thümmeler, F. (1994) In: The phytochrome chromophore. Kendrick, R. E. and Kronenberg, G. H. M., editors. *Photomorphogenesis in plants, 2nd edition*, Kluwer Academic Publishers, Dordrecht
3. Hübschmann, T., Börner, T., Hartmann, E., and Lamparter, T. (2001) *Eur.J.Biochem.* **268**, 2055-2063
4. Frankenberg, N., Mukougawa, K., Kohchi, T., and Lagarias, J. C. (2001) *Plant Cell* **13**, 965-978
5. Bhoo, S. H., Davis, S. J., Walker, J., Karniol, B., and Vierstra, R. D. (2001) *Nature* **414**, 776-779
6. Oberpichler, I., Molina, I., Neubauer, O., and Lamparter, T. (2006) *FEBS Lett* **580**, 437-442
7. Blumenstein, A., Vienken, K., Tasler, R., Purschwitz, J., Veith, D., Frankenberg-Dinkel, N., and Fischer, R. (2005) *Current Biology* **15**, 1833-1835
8. Lamparter, T., Michael, N., Mittmann, F., and Esteban, B. (2002) *Proc.Natl.Acad.Sci.U.S.A.* **99**, 11628-11633
9. Lamparter, T., Carrascal, M., Michael, N., Martinez, E., Rottwinkel, G., and Abian, J. (2004) *Biochemistry* **43**, 3659-3669
10. Wagner, J. R., Brunzelle, J. S., Forest, K. T., and Vierstra, R. D. (2005) *Nature* **438**, 325-331
11. Rüdiger, W., Thümmeler, F., Cmiel, E., and Schneider, S. (1983) *Proc.Natl.Acad.Sci.U.S.A.* **80**, 6244-6248
12. Rentsch, S., Hermann, G., Bischoff, M., Strehlow, D., and Rentsch, M. (1997) *Photochem.Photobiol.* **66**, 585-590
13. Heyne, K., Herbst, J., Stehlik, D., Esteban, B., Lamparter, T., Hughes, J., and Diller, R. (2002) *Biophys.J.* **82**, 1004-1016
14. Borucki, B., von Stetten, D., Seibeck, S., Lamparter, T., Michael, N., Mroginski, M. A., Otto, H., Murgida, D. H., Heyn, M. P., and Hildebrandt, P. (2005) *J.Biol Chem.* **280**, 34358-34364
15. van Thor, J. J., Borucki, B., Crielaard, W., Otto, H., Lamparter, T., Hughes, J., Hellingwerf, K. J., and Heyn, M. P. (2001) *Biochemistry* **40**, 11460-11471
16. Eilfeld, P. and Rüdiger, W. (1985) *Zeitschrift für Naturforschung C-A Journal of Biosciences* **40**, 109-114
17. Chen, E., Lapko, V. N., Lewis, J. W., Song, P. S., and Kliger, D. S. (1996) *Biochemistry* **35**, 843-850
18. Inomata, K., Hammam, M. A. S., Kinoshita, H., Murata, Y., Khawn, H., Noack, S., Michael, N., and Lamparter, T. (2005) *J.Biol.Chem.* **280**, 24491-24497

19. Andel, F. I., Murphy, J. T., Haas, J. A., McDowell, M. T., van der Hoef, I., Lugtenburg, J., Lagarias, J. C., and Mathies, R. A. (2000) *Biochemistry* **14**, 2667-2676
20. Mroginski, M. A., Murgida, D. H., von Stetten, D., Kneip, C., Mark, F., and Hildebrandt, P. (2004) *J.Amer.Chem.Soc.* **126**, 16734-16735
21. Andel, F., Lagarias, J. C., and Mathies, R. A. (1996) *Biochemistry* **35**, 15997-16008
22. Karniol, B. and Vierstra, R. D. (2003) *Proc.Natl.Acad.Sci.U.S.A.* **100**, 2807-2812
23. Giraud, E., Fardoux, J., Fourier, N., Hannibal, L., Genty, B., Bouyer, P., Dreyfus, B., and Vermeglio, A. (2002) *Nature* **417**, 202-205
24. Giraud, E., Zappa, S., Jaubert, M., Hannibal, L., Fardoux, J., Adriano, J. M., Bouyer, P., Genty, B., Pignol, D., and Vermeglio, A. (2004) *Photochem.Photobiol.Sci.* **3**, 587-591
25. Tasler, R., Moises, T., and Frankenberg-Dinkel, N. (2005) *FEBS J.* **272**, 1927-1936
26. Starostzik, C. and Marwan, W. (1995) *FEBS Lett.* **370**, 146-148
27. Falk, H. (1989) *The chemistry of linear oligopyrroles and bile pigments*, Wien Ed., Springer Verlag, Berlin, Heidelberg, New York
28. Lamparter, T. and Michael, N. (2005) *Biochemistry* **44**, 8461-8469
29. Scheerer, P., Michael, N., Park, J. H., Noack, S., Förster, C., Hammam, M. A. S., Inomata, K., Choe, H. W., Lamparter, T., and Krauß, N. (2006) *Journal of Structural Biology* **153**, 97-102
30. Kakiuchi, T., Kato, H., Jayasundera, K. P., Higashi, T., Watabe, K., Sawamoto, D., Kinoshita, H., and Inomata, K. (1998) *Chem.Lett.* 1001-1002
31. Kakiuchi, T., Kinoshita, H., and Inomata, K. (1999) *Synlett Sp Iss* **1999**, 901-904
32. Sawamoto, D. and Inomata, K. (2001) *Chem.Lett.* 588-589
33. Takeda, S., Jayasundera, K. P., Kakiuchi, T., Kinoshita, H., and Inomata, K. (2001) *Chem.Lett.* 590-591
34. Kinoshita, H., Hammam, M. A. S., and Inomata, K. (2005) *Chem.Lett.* **34**, 800-801
35. Hammam, M. A. S., Murata, Y., Kinoshita, H., and Inomata, K. (2004) *Chem.Lett.* **33**, 1258-1259
36. Hammam, M. A. S., Nakamura, H., Hirata, Y., Khawn, H., Murata, Y., Kinoshita, H., and Inomata, K. (2006) *Bull.Chem.Soc.Jpn.* **79** (in press)
37. Giraud, E., Vuillet, L., Hannibal, L., Fardoux, J., Zappa, S., Adriano, J. M., Berthomieu, C., Bouyer, P., Pignol, D., and Verméglio, A. (2005) *J.Biol.Chem.* **280**, 32389-32397
38. Yeh, K. C., Wu, S. H., Murphy, J. T., and Lagarias, J. C. (1997) *Science* **277**, 1505-1508
39. Falk, H., Müller, N., and Wöss, H. (1987) *Monatshefte fur Chemie* **118**, 1301-1315

40. Brünger, A. T., Adams, P. D., Clore, G. M., DeLano, W. L., Gros, P., Grosse-Kunstleve, R. W., Jiang, J. S., Kuszewski, J., Nilges, M., Pannu, N. S., Read, R. J., Rice, L. M., Simonson, T., and Warren, G. L. (1998) *Acta Crystallographica Section D: Biological Crystallography* **54**, 905-921
41. Baker, N. A., Sept, D., Joseph, S., Holst, M. J., and McCammon, J. A. (2001) *Proc.Natl.Acad.Sci.U.S.A* **98**, 10037-10041
42. DeLano, W. L. The PyMOL Molecular Graphics System. DeLano Scientific, San Carlos, CA, USA. <http://www.pymol.org>. 2002. <http://www.pymol.org>, DeLano Scientific, San Carlos, CA, USA
43. Dugave, C. and Demange, L. (2003) *Chem. Rev.* **103**, 2475

FOOTNOTES

*This work was supported by Deutsche Forschungsgemeinschaft, Sfb 498, TP B2 (T.L. and N.K.) and by Grant-in-Aid for Scientific Research (B) (No. 15350021) from Japan Society for the Promotion of Science (K.I.).

¹The abbreviations used are: λ_{\max} , wavelength of the absorption maximum; BV, biliverdin; DFT, density functional theory; GAF domain, abbreviation derived from cGMP-specific phosphodiesterases, cyanobacterial adenylate cyclases, and transcription activator FhlA; PAS domain, abbreviation derived from PER ARNT SIM; PLD, PAS-like domain; PCB, phycocyanobilin; P Φ B, phytochromobilin; Pfr, far-red-absorbing form of phytochrome; Pnr, near-red absorbing form of phytochrome; Pr, red-absorbing form of phytochrome; SEC, size-exclusion chromatography

FIGURE LEGENDS

Fig. 1. Chromophores used in the present study.

Fig. 2. Assembly of Agp1 with 5Za and 5Zs chromophores, UV/vis spectroscopy. Spectra during the initial 51 min after mixing chromophore and protein, recorded in 5 min intervals, are presented (black lines). The direction of absorption changes is indicated by arrows; the spectra of free chromophores in assembly buffer are shown by the grey lines.

Fig. 3. Time course of absorbance changes during assembly of Agp1 with all chromophores given in Fig. 1. The values for 5Za and 5Zs were taken from spectra as given in Fig. 2, and the values for 15Z/E a/s from spectra that were published previously (18).

Fig. 4. Photoconversion of Agp1 adducts with 18EtBV (a), 5Za (b) and 5Zs (c). Spectra were recorded after dark assembly (black line) or after irradiating the samples for 10 min with red light (655 nm light emitting diode, 50 $\mu\text{mol m}^{-2} \text{s}^{-1}$; grey line). The "dark minus red" difference spectra are given by the dashed lines.

Fig. 5. Size exclusion profiles of BV-, 5Za-, and 5Zs-Agp1-M15 adducts without (dark) or after red light treatment (red). The absorbance values were normalized in such a way that the areas under the curves are identical.

Fig. 6. Assembly of Agp2 with all chromophores given in Fig. 1. Spectra during the initial 51 min after mixing chromophore and protein, recorded in 5 min intervals, are presented (black lines). The direction of absorption changes is indicated by an arrow; the spectra of free chromophores in assembly buffer are shown by the grey lines. The BV and 18EtBV assembly is characterized by complex absorption changes (see also Fig. 7). The first spectra after mixing chromophore and protein are recognized by a high Pr absorption in the 700 nm region. The two arrows in these panels indicate the decrease of Pr (down arrow) and increase of Pfr absorption (up arrow) over time. Spectra of free chromophores are always clearly distinct from the spectra that were obtained after mixing with the protein.

Fig. 7. Time course of absorbance changes during assembly of Agp2 with BV and 18EtBV.

Fig. 8. Time course of absorbance changes during assembly of Agp2 with locked chromophores.

Fig. 9. Photoconversion of Agp2 adducts with (a) BV, (b) 18EtBV, (c) 5Za and (d) 5Zs. Spectra were recorded after dark assembly (black line) or after irradiating the samples for 10 min with either red light as

given in the legend of Fig. 4 (c,d) or with far-red light (a,b; 785 nm laser diode, ca. 100 $\mu\text{mol m}^{-2} \text{s}^{-1}$). The "dark minus red" or "dark minus far-red" difference spectra are given by the dashed lines.

Fig. 10 (a-c): Phytochrome chromophore binding pockets in the models of adducts with 5Za, 5Zs and BV. Semitransparent view of a section of the electrostatic surface area with chromophores and two amino acid residues in stick representation. Initial models of 5Za and 5Zs were generated using ViewerPro 4.2 (Accelrys, San Diego, USA). Initial models of the adducts with 5Za and 5Zs were obtained by replacing BV in the chromophore binding domain of *Deinococcus radiodurans* phytochrome DrBphP (PDB entry 1ZTU).

The amino acid labelling refers to the position within DrBphP (first number) and Agp1 (second number). The models were minimized using the program CNS (40). Negatively and positively charged surface areas are coloured in red and blue, respectively. Electrostatic surface potentials were calculated using the program APBS (41) with the nonlinear Poisson-Boltzmann equation and contoured at ± 3 kT/e. The figure was generated using PyMOL (42). (d) Superposition of 5Za (carbon atoms in green), 5Zs (carbon atoms in red) and BV (carbon atoms in grey) of (a-c).

The following amino acids of DrBphP are located within a 4 Å distance from the BV chromophore: C24, E27, I29, **M174**, **F198**, F203, **S206**, D207, I208, P209, A212, Y216, R254, **T256**, S257, **M259**, H260, M267, S272, **L273**, S274, H290. Homologous Agp1 amino acids are: C20, E23, I25, **L164**, **Y188**, F193, **G196**, D197, I198, P199, A202, Y206, R244, **V246**, S247, **V249**, H250, M257, S260, **M263**, S264, H280 (variant amino acids given in bold)

Figure 11. Proposed stereochemistry of the Agp1 and Agp2 chromophores during conversion of Pr to Pfr. Step 1 is the rapid C15=C16 *Z* to *E* isomerization, leading to the lumi-R photoproduct. During the conversion from lumi-R to Pfr (step 2), the stereochemistry of the C5 methine bridge is changed. This can involve either a rotation around the C5-C6 single bond (from *syn* to *anti*) and/or a *Z* to *E* isomerization of the C4=C5 double bond (a Hula-Twist mechanism) (43). Two different possibilities are drawn here.

TABLES

Table 1. Summary of dark reversion and photoconversion of Agp1 adducts. The Agp1 apoprotein was assembled with the chromophores as indicated in the first column. Photoconversion and dark conversion were measured at 702 nm, 690 nm, 672 nm and 692 nm for the BV-, 18EtBV-, 5Za- and 5Zs-adducts, respectively. The following light sources were used for photoconversion: 655 nm light emitting diode with $135 \mu\text{mol m}^{-2} \text{s}^{-1}$; 785 nm laser diode with $70 \mu\text{mol m}^{-2} \text{s}^{-1}$; 608 nm halogen light and interference filter with $45 \mu\text{mol m}^{-2} \text{s}^{-1}$.

chromophore	direction of dark reversion	light sources for photoconversion	initial rate of reversion	
			in darkness	with light
BV	from Pfr to Pr	Pr to Pfr photoconversion with 655 nm; back conversion with 785 nm	$2.2 \cdot 10^{-3} \text{ s}^{-1}$	$4.7 \cdot 10^{-3} \text{ s}^{-1}$
18EtBV	from Pfr to Pr	Pr to Pfr photoconversion with 655 nm; back conversion with 785 nm	$1.6 \cdot 10^{-4} \text{ s}^{-1}$	$5.8 \cdot 10^{-4} \text{ s}^{-1}$
5Za	from Pfr-like to Pr	Pr to Pfr-like photoconversion with 655 nm; back conversion with 785 nm	$5.0 \cdot 10^{-3} \text{ s}^{-1}$	$4.5 \cdot 10^{-3} \text{ s}^{-1}$
5Zs	from Pnr to Pr	Pr to Pnr photoconversion with 655 nm; irradiation of Pnr with 608 nm	$3.3 \cdot 10^{-4} \text{ s}^{-1}$	$1.7 \cdot 10^{-4} \text{ s}^{-1}$

Table 2. Summary of dark reversion and photoconversion of Agp2 adducts. The Agp2 apoprotein was assembled with the chromophores as indicated in the first column. Photoconversion and dark conversion of BV- and 18EtBV-adducts were measured at 755 and 740 nm, respectively; the 5Za- and 5Zs-adducts were measured at 640 and 692 nm, respectively. Light sources for photoconversion were as in Table 1. In the case of the 5Za-adduct, the rate of dark reversion or photoconversion could not be determined due to low absorbance changes ("n.a."= not applicable).

chromophore	direction of dark reversion	light sources for photoconversion	initial rate of reversion	
			in darkness	with light
BV	from Pr to Pfr	Pfr to Pr photoconversion with 785 nm; back conversion with 655 nm	$1.2 \cdot 10^{-2} \text{ s}^{-1}$	$6.2 \cdot 10^{-2} \text{ s}^{-1}$
18EtBV	from Pr to Pfr	Pfr to Pr photoconversion with 785 nm; back conversion with 655 nm	$3.8 \cdot 10^{-3} \text{ s}^{-1}$	$1.4 \cdot 10^{-1} \text{ s}^{-1}$
5Za	n.a.	Pr to Pfr-like photoconversion with 655 nm; back conversion with 785 nm	n.a.	n.a.
5Zs	from Pnr to Pr	Pr to Pnr photoconversion with 655 nm; irradiation of Pnr with 608 nm	$3.2 \cdot 10^{-4} \text{ s}^{-1}$	$1.2 \cdot 10^{-3} \text{ s}^{-1}$

FIGURES

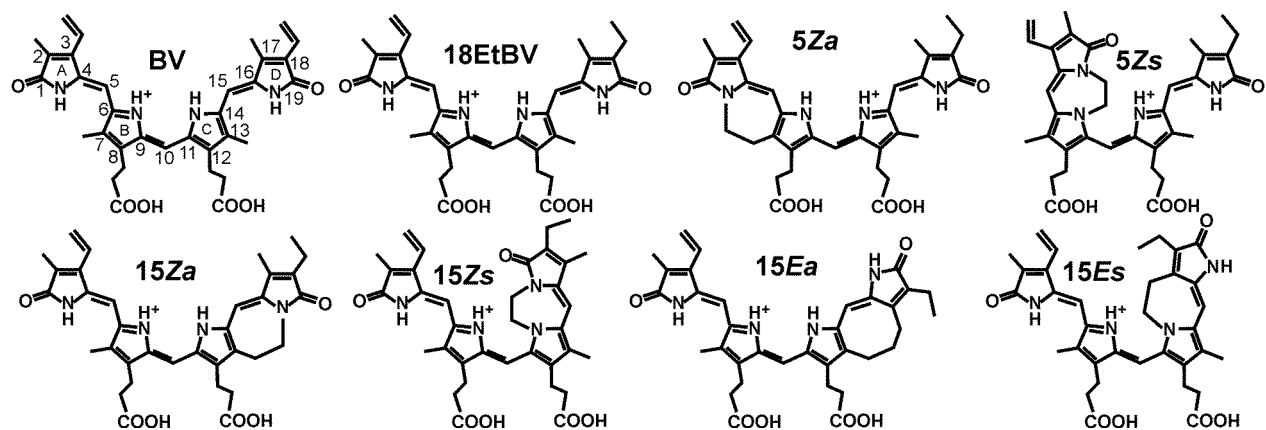


Figure 1

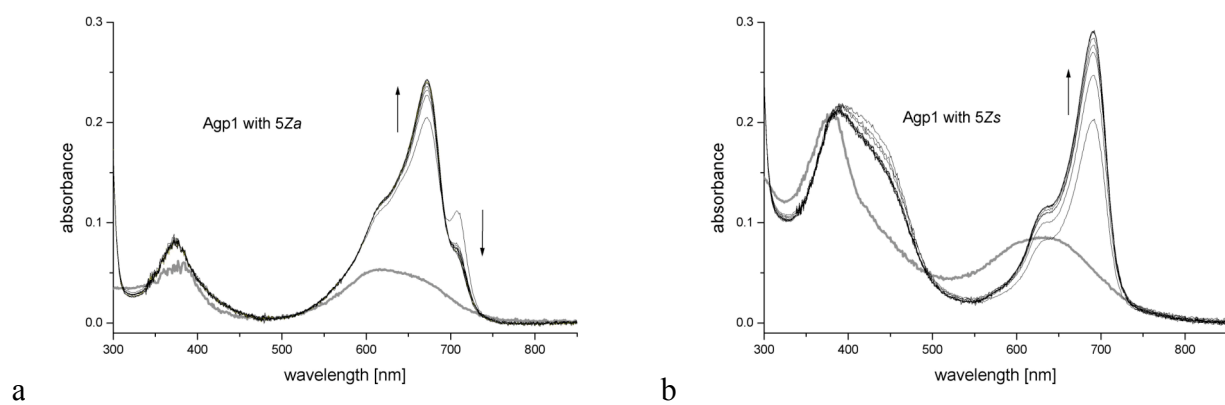


Figure 2

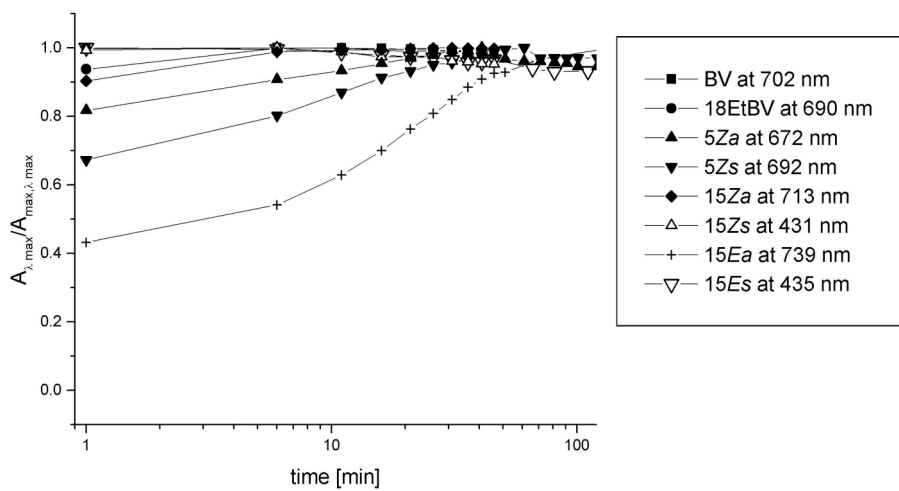


Figure 3

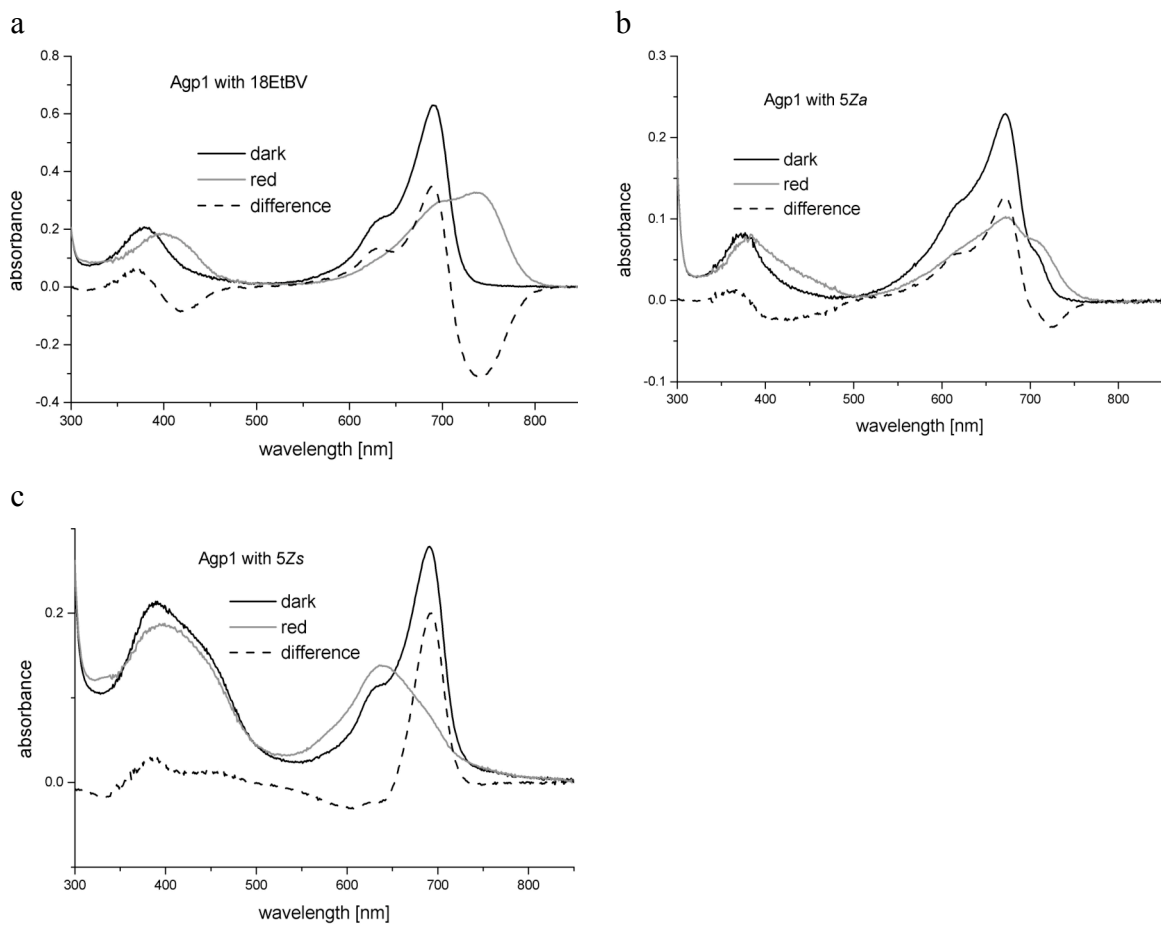


Figure 4

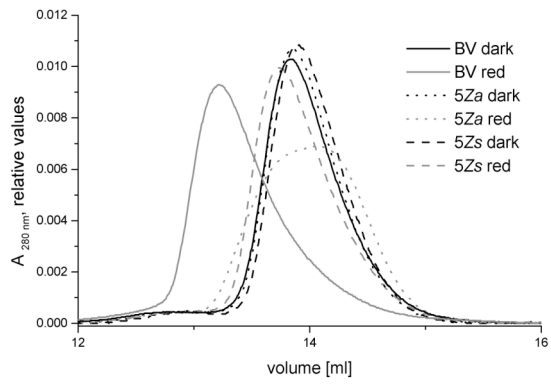


Figure 5

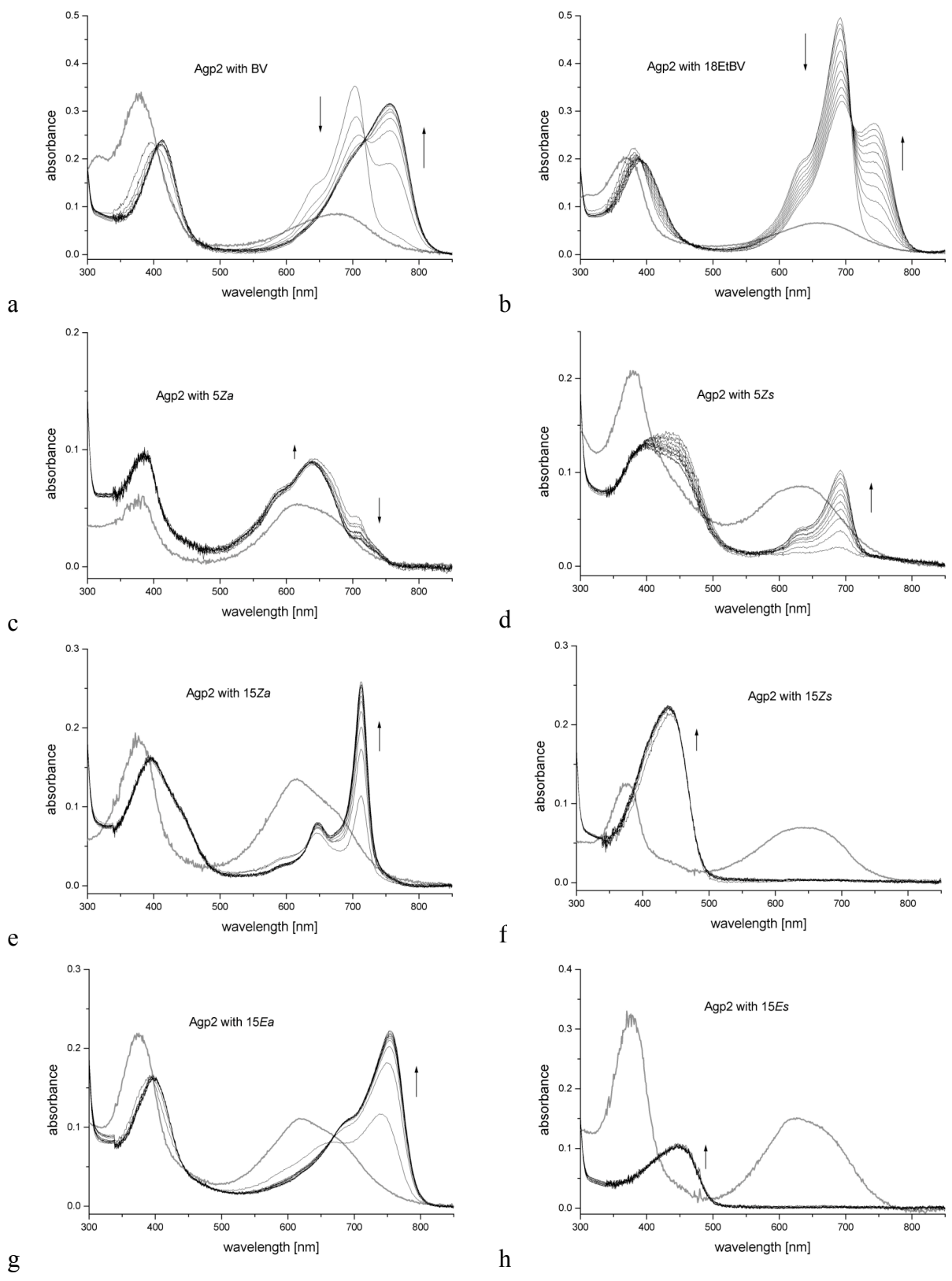


Figure 6

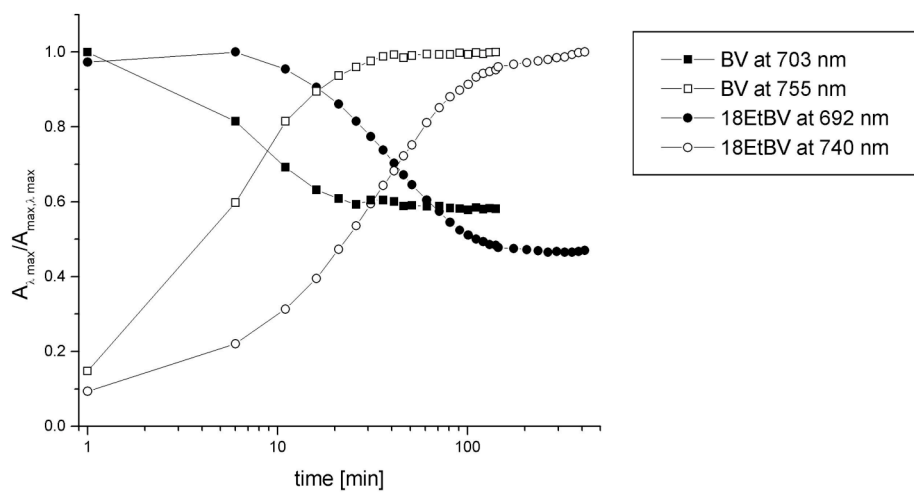


Figure 7

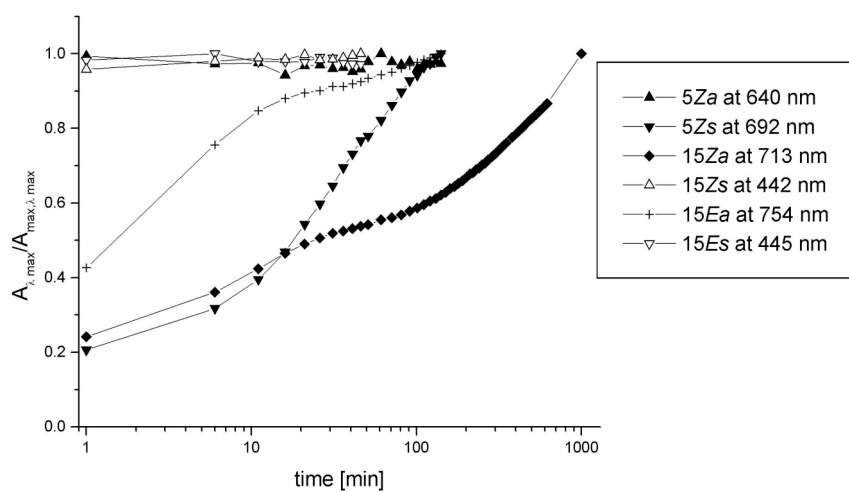


Figure 8

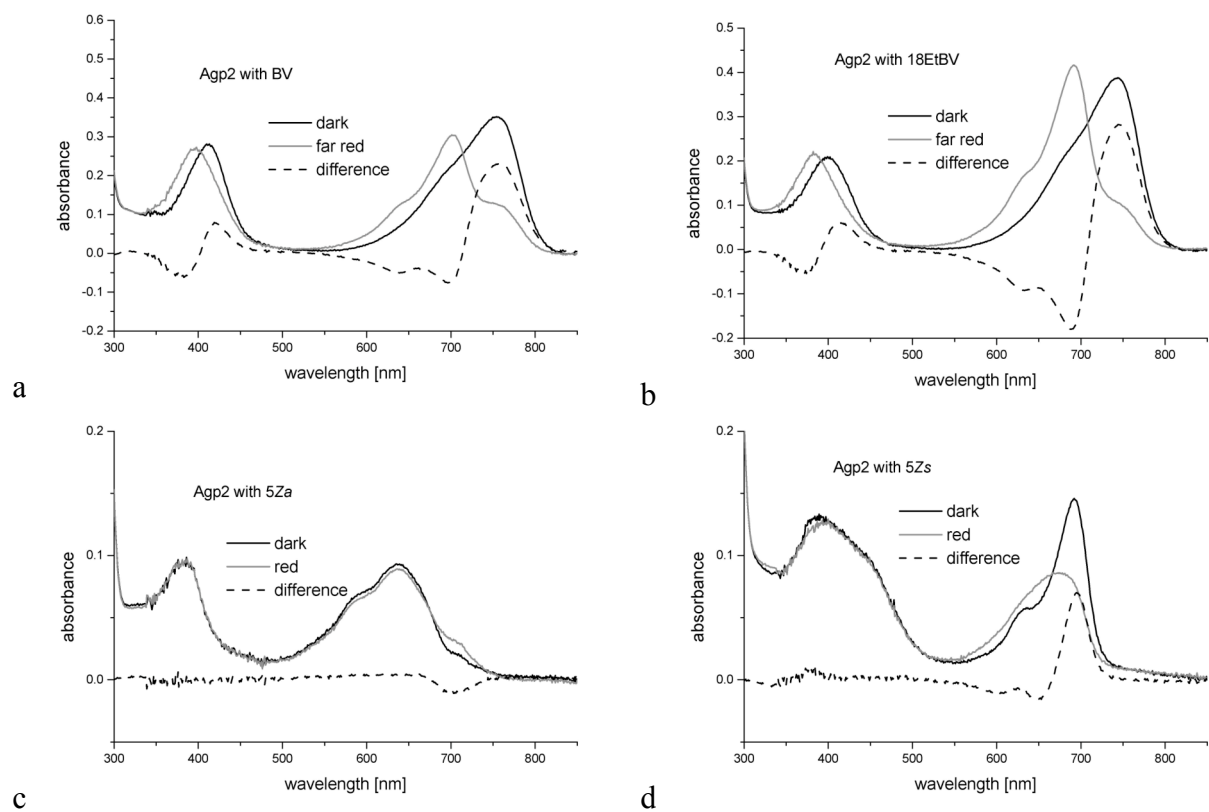


Figure 9

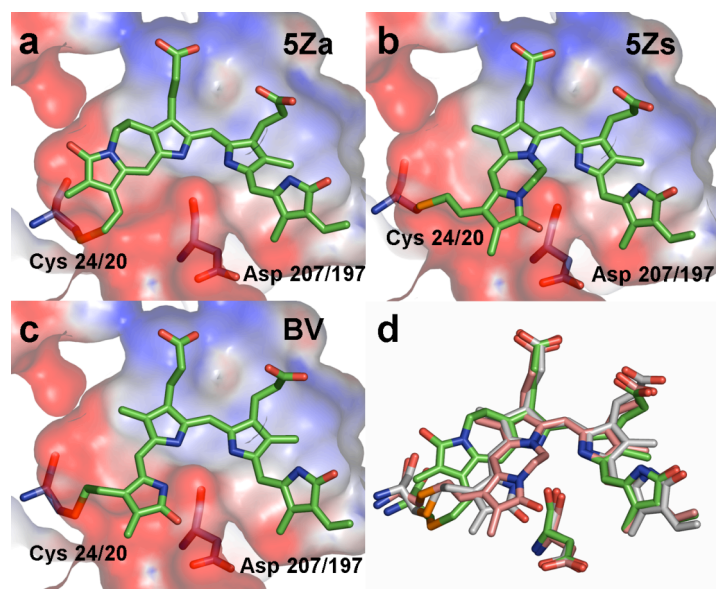


Figure 10

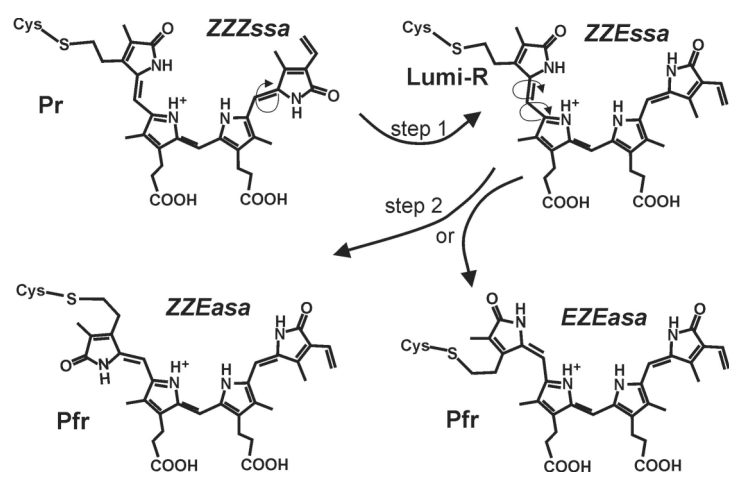


Figure 11